

## Stress intensity factors in crack closure problems

ENESCU IOAN  
Department of Mechanical Engineering  
Transylvania University of Brasov  
500036 Bvd. Eroilor nr.29, Brasov, ROMANIA  
enescu@unitbv.ro

*Abstract:* In the paper are shown the rising expectations in the design of mechanical elements generate a need to incorporate, in more accurate ways, aspects that were previously solely approximated, or not even taken into consideration. Such is the case of the crack fatigue and propagation problems, both relevant when estimating the lifespan of a mechanical element that is subject to alternating loads, or that has initial cracks of certain extension.

*Key-Words:* linear elasticity, boundary conditions, system structure.

### 1 Introduction

In Linear Elastic Fracture Mechanics (LEFM), the most used parameter in terms of determining the cyclic fatigue life or the unstable nature of a process of monotonic loads is the Stress Intensity Factor (SIF). Many work studies are dedicated to the presentation of this parameter's values in different situations and to the specific programs developed in order to obtain it both in finite elements and in boundary elements.

However, the majority of such studies focus on cases in which the crack lips are almost completely open and smooth, respectively with a null crack friction coefficient. This case, that can result very relevant when it comes to predominant one mode problems or in metals, becomes less relevant in mixed mode problems, especially in the anisotropic materials and composites. Due to the increasing use of this types of materials – like concrete, and especially fiber composites – this problem becomes one of unique importance and of great essence, if we take into

$$C_{ik}u_i(Q) = \int_{\partial\Omega} U_{ik}(Q,P)t_i(P)d\partial\Omega - \int_{\partial\Omega} T_{ik}(Q,P)u_i(P)d\partial\Omega + \int_{\partial\Omega} U_{ik}(Q,P)X_i(P)d\Omega \quad (2.1)$$

where  $U_{ik}$  is the Kelvin fundamental solution of the Navier's equations,  $T_{ik}$  are tractions corresponding to those fundamental solution of the Navier's equations,  $T_{ik}$  are the tractions corresponding to those fundamental solutions (the expressions for the orthopic case are included in the Appendix), and  $C_{ik}$  can be expressed as:<sup>9</sup>

account (1) the dramatic reduction that the consideration of such factors might lead to for the stress intensity factor and for the predicted cyclic fatigue life, and (2) the possible lack of crack propagation in situations in which a simple calculation of an open crack factor indicated a crack propagation. This is mainly the case of mode II cracks with increased friction between the crack lips.

### 2 Formulation of the beam in 2-nd linear elastically multi domain problems

The first equation of the BEM, in its direct formulation, is the well-known Somigliana's identity, which expresses the displacement vector  $u_i(Q)$  of a point Q of a domain  $\Omega$  as a function of the displacements  $u_i(P)$  and tractions  $t_i(P)$  of the boundary points of this dominium and the body forces  $X_i$

$$C_{ik} = \begin{cases} \delta_{ik} \rightarrow Q \in \Omega \\ C'_{ik} \rightarrow Q \in \partial\Omega \\ 0 \rightarrow Q \notin \Omega \cup \partial\Omega \end{cases} \quad (2.2a)$$

with

$$C'_{ik} = \frac{1}{4\pi(1-\nu)} \times \begin{bmatrix} 2(1-\nu)(\pi + \alpha_1 - \alpha_2) & \text{sen}^2 \alpha_1 - \text{sen}^2 \alpha_2 \\ + \frac{1}{2(\text{sen}2\alpha_1 - \text{sen}2\alpha_2)} & \\ \text{sen}^2 \alpha_1 - \text{sen}^2 \alpha_2 & 2(1-\nu)(\pi + \alpha_1 - \alpha_2) \\ - \frac{1}{2}(\text{sen}2\alpha_1 - \text{sen}2\alpha_2) & \end{bmatrix} \quad (2.2b)$$

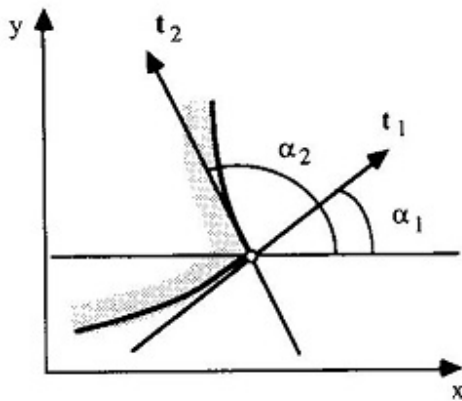


Fig.1 Geometrical mean of  $\alpha_1$  and  $\alpha_2$

where  $U_{ik}$  is the fundamental solution of the Navier equation,  $T_{ik}$  are the tractions corresponding to the mentioned fundamental solution, included in the Appendix on the orthotropic case, and  $C_{ik}$  can be expressed as formula (2) for isotropic materials, where  $\alpha_1$  and  $\alpha_2$  have the geometrical meaning shown in Figure 1,  $\delta_{ik}$  is the Kronecker tensor,  $\mathbf{r}$  the radio vector joining the points P and Q,  $n$  the outward normal to the boundary at point P and  $\nu$  the Poisson

$$C_{ik} u_i(Q) = \sum_{j=1}^{Ne} \int_{\partial\Omega_j} U_{ik}(Q,P) \left[ \sum_{m=1}^{Nnj} (t_i^j)_m \varphi_m \right] d\partial\Omega_j - \sum_{j=1}^{Ne} \int_{\partial\Omega_j} T_{ik}(Q,P) \left[ \sum_{m=1}^{Nnj} (u_{ij})_m \varphi_m \right] d\partial\Omega_j \quad (2.4)$$

With  $N_{nj}$  the number of nodes of element  $j$ , and  $\varphi_k$  the interpolation functions for 2-D continuous elements,

coefficient [for plane stress, this value must be modified by the well-known expression  $\nu^* = \frac{\nu}{1+\nu}$

Under some circumstances, the domain integral in (1) can be rewritten as the sum of two boundary integrals, in such a way that is possible to express the displacement of any point of the domain  $\Omega$  in terms of only boundary integrals. In this work, however, no body forces have been considered, hence such integral disappears, and the equation (1) is directly expressed based on the boundary integral function. (fig1)

If a boundary discretization with  $N_e$  elements is used, and the displacements and tractions are approximated inside each element in terms of nodal values, in the standard form of BEM, as (formula (2.3)

$$\begin{aligned} u_i^j &= \sum_{k=1}^{Nnj} (u_i^j)_k \varphi_k \\ t_i^j &= \sum_{k=1}^{Nnj} (t_i^j)_k \varphi_k \end{aligned} \quad (2.3)$$

where  $N_{nj}$  is the number of nodes of the element  $j$ , and  $\varphi_k$  the shape function for 2-D continuous elements, then the eq(2.1) can be approximated by

then equation (1) can be approximated by (formula 2.4)

For example, in the case of linear elements (two nodes per element), equation (4) can be rewritten as

$$\begin{bmatrix} C_{11} & C_{12} \\ C_{21} & C_{22} \end{bmatrix} \begin{bmatrix} u_1(k) \\ u_2(k) \end{bmatrix} + \sum_{j=1}^{Ne} \begin{bmatrix} A_{111}^{kj} & A_{211}^{kj} & A_{112}^{kj} & A_{212}^{kj} \\ A_{121}^{kj} & A_{221}^{kj} & A_{122}^{kj} & A_{222}^{kj} \end{bmatrix} \times \begin{bmatrix} (u_i^j)_1 \\ (u_i^j)_2 \\ (u_i^j)_3 \\ (u_i^j)_4 \end{bmatrix} = \sum_{j=1}^{Ne} \begin{bmatrix} B_{111}^{kj} & B_{211}^{kj} & B_{112}^{kj} & B_{212}^{kj} \\ B_{121}^{kj} & B_{221}^{kj} & B_{122}^{kj} & B_{222}^{kj} \end{bmatrix} \begin{bmatrix} (t_i^j)_1 \\ (t_i^j)_2 \\ (t_i^j)_3 \\ (t_i^j)_4 \end{bmatrix} \quad (2.5)$$

If this expression is applied to each of the nodes and the corresponding boundary conditions are also included, it is possible to compute an algebraic linear system with  $[2\sum_j(Nnj-1)]$  equations and unknowns, corresponding to the displacements and tractions of the boundary nodes.

If the collocation point is not one of the nodes of the element along which the integrals in (5) are computed, a standard Gauss-Legendre quadrature is used. On the other hand, when it is placed from a node inside the adjacent element, singular integrands appear in the integrals of (5). In this case, the constants  $B$  are computed by using a quadrature with logarithmic weight function, while the constants  $A$  are computed, together with the free term  $C_{ik}$ , by imposing a rigid body condition to the studied body. At each node two equations and six unknowns (two displacements, and two tractions for each of the elements to which the node belongs) can then be established. Most of the times, these tractions are expressed in local coordinates being necessary to transform the traction vector based on these coordinates.

Ultimately, once the coefficient and independent term vector matrix is assembled, and the boundary conditions are applied, an algebraic system is obtained in the form (2.6):

$$K_x = f \quad (2.6)$$

in which the unknowns,  $x$ , correspond to boundary displacements and/or tractions. The solution of this system is performed by any standard method, depending on its size.

Once the unknown displacements and tractions have been obtained, the displacements of any internal point are also obtained by (1), while the stresses may be computed by applying the stress operator to it. Focusing solely on the contact problem formulation between to elastic solids, with their interface initially

(formula 2.5a, 2.5b)

in a full contact, and normal for both solids. This is the only case of interest for this context. The non-traction condition for the mentioned point and with the data (typology of zone) described in Figure 2 is expressed as

$$u_N \leq 0 \quad (2.7)$$

Where  $u_N$  is the projection of relative displacement between equivalent points (equal to the post-contact position) above normal.

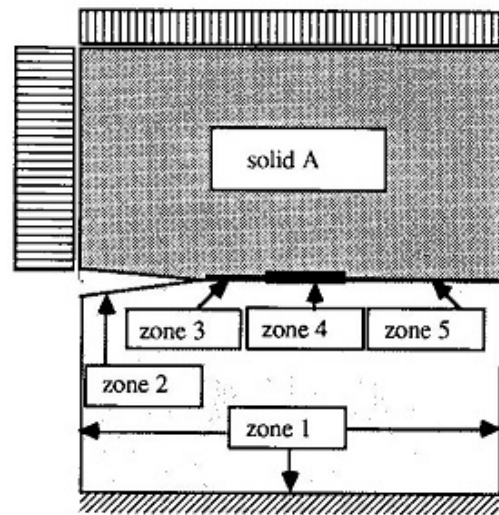


Fig.2 Typology of zone.

The static boundary conditions, in the unilateral case proposed in this work and based on the Coulomb's Law of Friction like the one used here, can be expressed as formula 2.7

Besides that, the compatibility and equilibrium conditions are to be met between the two solids, in the points in which contact has been established. For this, the following different areas are defined in terms of the global boundary of each solid (Figure 2.)

- No contact area (area no. 1) – the area that shall never establish contact
- Candidate to contact area (area no. 2) – the area that still has not established a contact, that might establish one at a specific load level.

- Slip area (area no. 3) –  $|r = \mu\sigma_N|$
- Adherent area (area no. 4) –  $|r < \mu\sigma_N|$
- Welding area (area no. 5) – the contact area in which both solids are considered welded, thus recognizing the traction stresses.

The contact problem between two solids, or better said between two domains of one body, as in this case, consists therefore in approaching the BEM equations to each contact solid, including implicitly or explicitly (in this case the second option was chosen) the boundary conditions (compatibility and equilibrium) in the contact area for each load level, as well as the boundary conditions in the other areas for each one of the aforementioned solids.

The program that has been implemented includes linear, quadratic and quarter-point-singular-traction elements (– 1/2 singularity), all of them with stresses and displacement continuity, as long as area no. 1 is checked for special nodes (nodes with excess or no unknowns), treated in an analogue mode in [2]. In case of friction, the friction coefficient is defined independently for each element, as it is possible to have independent contact areas between two solids with different friction coefficients.

### 3 Equation system structure and problem solving

Given the non-linear character of the contact problem, and independent of the solving method

$$\begin{aligned} &K_{LL}^S \cdot x_L^S + K_{LC}^S \cdot x_C^S = V_L^S \\ \rightarrow [K_{CC}^S - K_{CL}^S \cdot (K_{LL}^S)^{-1} \cdot K_{LC}^S] \cdot x_C^S &= V_C^S - K_{CL}^S (K_{LL}^S)^{-1} V_L^S \\ &K_{CL}^S \cdot x_L^S + K_{CC}^S \cdot x_C^S = V_C^S \end{aligned} \tag{3.1}$$

with S=A, B;  $x_L$  unknowns to be eliminated, and  $x_C$  the corresponding to the candidate to contact zone. Equations (3.1) can also be expressed as

$$\bar{K}^S \cdot x_C^S = \bar{V}^S \tag{3.2}$$

Each one of the  $K^S$  matrixes is a  $2n \times 6n$  with  $n$  the number of nodes of the contact area. In fact, there are two integral equations for each solid, for each node as collocation point, and each node of the contact area with 6 unknowns (2 displacements and 2 tractions in each of its previous and subsequent elements), identified as  $u_1, u_2, \sigma_{ant}, \tau_{ant}, \sigma_{pos}, \tau_{pos}$ .

chosen: incremental, iterative or incremental-iterative, it is necessary to build and solve several times a linear equation system, in order for the major execution time would match this process. Therefore, it is very important to choose the corresponding algorithm to use in order to reduce this time as much as possible.

When selecting the system's basic unknowns, two possibilities arise. The first one is selecting explicitly the necessary unknowns, in order for the problem to be solved just by merely applying the integral equations. In other words, instance, both the boundary conditions and the compatibility and equilibrium equations in the contact area are included by default without appearing in the final system. In this way, the number of equations is reduced, but it is necessary to proceed with building the constants of integration for each step, given that these basic unknowns alternate in each iteration once the contact conditions modify in all steps. This involves the necessity to archive the corresponding contact area-related constants; given that recalculating the latter would result totally inefficient.

The first step to complete (if necessarily), regardless of the chosen process, uses to be the compression of the unknowns belonging to the nodes outside the contact area. For this, a boundary element standard process must be independently applied for each of the two solids, taking into consideration the following for each of them (formula 3.1)

Finally, it is necessary to add to the previous equations 8 equations for each contact node corresponding to the contact conditions (the  $K^{AB}$  matrix) and node type-dependent. For example, for a 44 node, those would be expressed as (formula 3.2)

$$\begin{aligned} u_1^A &= u_1^B \quad u_2^A = u_2^B \quad \sigma_{ant}^A = \sigma_{pos}^A \\ \tau_{ant}^A &= \tau_{pos}^A \quad \sigma_{pos}^B = \sigma_{ant}^B \quad \tau_{pos}^B = \tau_{ant}^B \tag{3.3} \\ \tau_{ant}^A &= \tau_{pos}^B \quad \tau_{ant}^B = \tau_{pos}^A \end{aligned}$$

The implemented structure for the matrix can be seen in Figure 5, with matrixes  $K^A, K^{AB}, K^B$  as the only matrixes archived.

With regard to the solving process, the Gauss elimination process is used, but with a pretriangulation of matrixes  $\mathbf{K}^A$  and  $\mathbf{K}^B$ , the ones kept unaltered throughout the entire process, with pivot on the rows. This said, in each incremental step, this can be performed by simply solving a very easy and multiple zeroed  $6n \times 6n$  equation system ( $4n \times 4n$  on the first assembly alternative, when the mandatory traction continuity is taken into consideration).

Solving a contact problem with friction requires knowing the history of the entire process, given its irreversible character. This implies the necessity to follow an incremental process for the solution. On the other hand, in a contact problem without friction, with an unknown contact area, an iterative process can be followed for its computation, and in order to

establish the contact stress distribution. Finally, in a contact problem without friction and with an *a priori* known contact area, a single load process enables determining its stress distribution.

The only general procedure is, therefore, an incremental process, the one used in this work.

## 4 Results

The first example corresponds to the case solved by Woo et al, through a complex variable procedure, of a quadratic plate subjected to pure bending corresponding to a bending moment equaling  $2/3$  and to a variable crack length. Due to this load, a partial crack closure occurs on the compression side and a crack opening on the traction.

Table 1.

a	0.1	0.2	0.3	0.4	0.5	0.6	0.7
l	0.025	0.05	0.05	0.05	0.05	0.1	0.1
F(obt)	0.05	0.101	0.151	0.203	0.258	0.324	0.402
Dif%	0.04	0.85	0.21	0.1	0.31	0.39	0.3
a*(obt)	0.0675	0.1375	0.20625	0.27	0.3482	0.41789	0.4875
a*(Woo)	0.0668	0.1344	0.2036	0.2749	0.3488	0.4255	0.5052
Dif(%)	0.69	1.53	0.86	1.2	0.11	1.21	2.39
F*(obt)	0.066	0.1302	0.20145	275060.	0.3465	0.4366	0.5418
F^(Woo)	0.0663	0.1344	0.2038	0.276	0.3529	0.4379	0.5403
F(Woo)	0.05	0.101	0.151	0.203	0.258	0.324	0.402
Dif(%)	0.3	2.14	0.77	0.23	1.22	2	0.18

The results obtained from the discretization are included in Table 1, consisting of 22 quadratic elements, 2 linear elements and 4 singular elements for each body. In addition, the length values of the initial crack  $a^*$ , the dimensionless SIF factors, without taking into consideration the crack closure, as the latter takes place at tip A, are also included.

$$F = \frac{K_I}{\sigma\sqrt{\pi a}} \quad F^* = \frac{K_I^*}{\sigma\sqrt{\pi a^*}}$$

Naturally, if the calculation is made regardless of the crack closure effect, the SIF at tip B becomes a negative value, indicating the occurrence of compressions. If the contact process is continued and the crack gets closed, finite compression stresses appear on edge B, which along with the singular stress distribution undertaken by the singular

elements give rise to a null SIF value corresponding to the real one.

The value included in the table for the actual contact length corresponds to the medium point of the elements where the compressive and traction conditions take place.

Finally, what needs to be highlighted within the above table is the good concordance with the results obtained by Woo, with differences found in all the cases below 3%.

The second case corresponds to a similar one that Ballarini et al studied in different conditions. This refers to the case of 2 side-quadratic sandstone subjected to the uniform tangential stress of a unit value on the upper half and fixed on the base. This involves a stage at the base that leads to a compression on the crack's tip B and the crack's partial closure, as well as to a case of traction, with the crack opening at tip A. The discretization has

been performed with 23 quadratic elements for each sub domain and 2 singular elements of a length  $l = 0,05$  situated at the crack's tips A and B, on the welding areas. Thus, the total number of nodes is 50 per each domain.

As such, the stress intensity factors (SIF) were obtained at tips A and B via the aforementioned method. Once more, the stresses at tip B are negative, but finite, given the lack of singularity; therefore if a type II singularity approximation is added, the  $K_I$  value should clearly become null, as in fact does occur.

In terms of the  $K_{II}$  present at that tip, if the adjacent area is under slip, which actually depends on the friction coefficient and the load level, again a singular distribution of the tangential stresses present on SIF will occur, different than zero on modes II. The value of  $K_{II}$  shall decisively depend on the friction coefficient. On the other hand, if found in adherence, the SIF in mode II of tip B shall be null, given the presence of a singularity at the tip of the adherence area – thus, clearly it is necessarily to redefine the mesh and include the singular elements on that area if the aim is to calculate it. In this example, the load value is sufficient for the tip B to be always slipping; therefore such modification is not needed.

As such, the stress intensity factors (SIF) were obtained at tips A and B via the aforementioned method. Once more, the stresses at tip B are negative, but finite, given the lack of singularity; therefore if a type II singularity approximation is added, the  $K_I$  value should clearly become null, as in fact does occur.

In terms of the  $K_{II}$  present at that tip, if the adjacent area is under slip, which actually depends on the friction coefficient and the load level, again a singular distribution of the tangential stresses present on SIF will occur, different than zero on mode II. The value of  $K_{II}$  shall decisively depend on the friction coefficient. On the other hand, if found in adherence, the SIF in mode II of tip B shall be null, given the presence of a singularity at the tip of the adherence area – thus, clearly it is necessarily to redefine the mesh and include the singular elements on that area if the aim is to calculate it. In this example, the load value is sufficient for the tip B to be always slipping; therefore such modification is not needed.

Table II presents the influence that the friction coefficient has on the stress intensity factors for a

crack with the initial length of 0,4. In case the crack closure is not taken into consideration, the dimensionless SIFs computed are the following:

$$F_I^A = \frac{K_I^A}{\sigma\sqrt{\pi a}} = 0.1889$$

$$F_I^B = -0.30944$$

$$F_{II}^A = 0.6575$$

$$F_{II}^B = 0.48993$$

were negative values now appear in the  $F_I^B$  factor because the contact process was not followed until reaching the predicted non-null value.

On the first position of this table it can be noticed that the effective crack length does not practically depend on the friction coefficient, remaining in any case equal to 0,2766. Moreover, the value of  $F_I^B$  remains invariable and essentially null ( $0,35 \times 10^{-3}$ ), whereas the values of  $F_I^A$  and  $F_{II}^A$  do not substantially change, in accordance with the fact that the actual length remains constant, and are slightly less than the result of  $F_I^A$  and  $F_{II}^A$  in case the closure by  $\sqrt{a}$  or  $a$  is not considered.

In this case, evidently, all the values change, including the length of the actual crack that may be regarded as representative for the geometrical conditions of the problem and of the specified load, as well as independent of the friction coefficient, given that these values extend to any of its other values. It should be emphasized that the crack length that leads to a SIF equal to its 0,4 length correspondent, regardless of the crack closure, is of approximately 0,65; in other words, 60% more than the coefficient initially expected, thus it is important to take into consideration this phenomena in cases of loads that generate this.

The third and last example indicates a simple flexion problem with the same dimensions and discretizations as the ones on the first example, and with the following values:  $\sigma_1 = 2$ ,  $\sigma_2 = 1$  and  $\tau = 0,25$ . Once more, singular elements were introduced either on the compression edge (B) or on the traction (A), so that the SIF in B shall be null after the contact process. The value of  $K_{II}^B$  depends, however, of the contact state (adherence or slip) existing on its proximities, and, as such, of the friction coefficient between the crack lips.

In the following tables, a variation of the actual dimensionless SIFs can be observed, defined as

$$F_I^A = \frac{K_I^A}{\sigma\sqrt{\pi a^*}}$$

with  $\sigma = 1,5$  and, analogically, for tip B and for the mode II SIF. In addition, to be noted the values of the actual crack length and the adherence  $d$  length, which if not null, leads to a  $F_{II}^B$  coefficient null value, as indicated.

## 5 Conclusions

A complete definition of the contact problem with small distortions and displacements was shown between the orthotropic environments by means of the BEM method, and its capabilities have been demonstrated, carrying important advantages in front of other means in this domain, especially in terms of studying crack closure problems.

Including singular elements facilitates in a simple way the determination of SIFs, including in cases of friction and in areas subject to compression, a null value being noticed in such cases, as expected.

It has been confirmed the necessity to incorporate the crack closure effects when establishing the SIFs strengths if such thing occurs, and the great importance of the friction coefficient on the mode II factors. On the other hand, the friction coefficient essentially does not affect the actual crack length and the SIFs in mode I.

No major influence has been noticed with regard to the non-isotropic properties on SIF values, at least when the orthotropic axes are aligned with the crack and its corresponding load, even though the mode II ones alter on high level

## References:

- [1] Alacon, E., Martin, A. & Paris, F., *Boundary elements in potential and elasticity theory, Computers and Structures*. 1979, **10**, pp.351-362.
- [2] Andersson, T., Frederiksson, B., & Allan Person, B.G., *The boundary element method applied to two dimensional contact problems*. New Dev. in B.E.M., ed. C.A. Brebbia CML Publ., 1980
- [3] Andersson, T., *The boundary element method applied to two-dimensional contact problem with friction*, in B.E.M. ed C. A. Brebbia, pp.239-258, Springer Verlag 1981
- [4] Andersson, T., Allan Person, B.G., *The boundary element method applied to two dimensional contact problems*, Progress in B.E.M. , ed. C.A. Brebbia, Vol2, Pentech Press, 1983
- [5] Barnerjer, P.K. , & Butterfield, R. Boundart, *Element Methods in Engineering Sciences*, Mc Graw Hill 1981.
- [6] Blandform, G.,E., Ingraffea, A., R., & Liggett, J.A., *Two dimensional stress intensity factor computation using the Boundary Element Method* , Int.J.for Num.Meth.in Eng., **17**, pp.387-404.
- [7] Brebbia, C.A. *The boundary Element Method for Engineers*, Pentech Press 1978.
- [8] Doblare., M., Esping.,F., & Garcia.L., *Determination de tensions de contacto entre materiales ortotropos mediante el M.E.C.*, Revista International der Methodos Numericos para Calculo y Diseno en Ingenieria, Vol.5, pp. 395-420.
- [9] Doblare . M., *Computational Aspects of the B.E.M.*, in Tropics in BE Research III, ed. C.A. Brebbia, pp. 51-131 Springer Verlang 1987.